



Enhanced photodegradation of antibiotics based on anoxygenic photosynthetic bacteria and bacterial metabolites: A sustainably green strategy for the removal of high-risk organics from secondary effluent

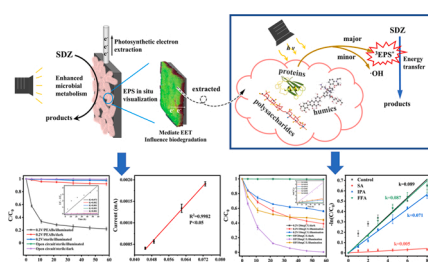
Mengmeng Zhao, Xiaoyan Bai, Yaping Zhang, Yong Yuan, Jian Sun*

Guangzhou Key Laboratory of Environmental Catalysis and Pollution Control, Guangdong Key Laboratory of Environmental Catalysis and Health Risk Control, School of Environmental Science and Engineering, Institute of Environmental Health and Pollution Control, Guangdong University of Technology, Guangzhou 510006, China

HIGHLIGHTS

- Photosynthetic electron extraction significantly enhanced SDZ biodegradation and stimulated EPS secretion.
- EPS extracted as a biomaterial can induce a complete removal of SDZ within 58 h.
- The biodegradation capabilities of PEABs were mainly affected by the contents of extracellular proteins.
- protein-like and humic substances secreted by photoheterotrophic metabolism may be the main photosensitive components in EPS.
- $^3\text{EPS}^*$ predominated the indirect photodegradation of SDZ.

GRAPHICAL ABSTRACT



ARTICLE INFO

Keywords:

Bioaugmentation technology
Photosynthetic electron extraction
Extracellular polymeric substances (EPS)
Eco-friendly biomaterial
Antibiotic

ABSTRACT

Antibiotic residues in effluents discharged from wastewater treatment plants (WWTPs) have been considered high-risk organics due to biorefractory property and potential toxicity. Secondary pollution and unsustainability existed in advanced treatment of secondary effluent are currently in urgent need of improvement. In this study, a sustainably green strategy based on *Rhodospirillum rubrum* (*R. rubrum*) by regulating the structure of extracellular polymeric substances (EPS) was proposed for the first time to achieve efficient removal of sulfadiazine (SDZ). Results showed that 0.2 V was the optimal external potential for *R. rubrum* to efficiently remove SDZ, where the biodegradation rate constant obtained at this potential was 4.87-folds higher than that in open-circuit mode and a complete removal was achieved within 58 h in the presence of EPS extracted at this potential. Three-dimensional excitation-emission matrix (3D-EEM) spectra analysis suggested that tryptophan protein-like, tyrosine protein-like, humic acid-like and fulvic acid-like substances present in EPS were the main effective components which were responsible for the indirect photodegradation of SDZ. The quenching experiments showed that $^3\text{EPS}^*$ was the dominant reactive species which accounted for 90% of SDZ removal. This study provides new implications for the advanced treatment of secondary effluent organic matters by developing eco-friendly bioaugmentation technology and biomaterials.

* Corresponding author.

E-mail address: sunjian472@163.com (J. Sun).

<https://doi.org/10.1016/j.jhazmat.2022.128350>

Received 23 November 2021; Received in revised form 13 January 2022; Accepted 23 January 2022

Available online 29 January 2022

0304-3894/© 2022 Elsevier B.V. All rights reserved.

1. Introduction

With the improvement of life qualities and medical conditions, antibiotics, as an effective antibacterial agent, have been used indiscriminately and frequently in daily life (Song et al., 2019; Langbehn et al., 2021). Of all antibiotics used in humans and animals, 30–90% are excreted unchanged or as active metabolites via urine and feces, and eventually converged in municipal wastewater treatment plants (WWTPs) through sewage pipe networks (Hanna et al., 2018). However, most of the antibiotics fail to be efficiently removed by traditional wastewater treatment processes and are released into the environment since pharmaceuticals are designed to be of high degree of stability and are inherent to induce physiological effects at low concentrations (Zhang et al., 2015; Hu et al., 2018; Michael et al., 2013). The presence of antibiotics in aquatic environments, even in traces, may lead to the spread of antibiotic-resistant bacteria, and bioaccumulation and biomagnification of antibiotic-resistant genes (ARGs) in organisms, thereby posing a potential threat to human health through drinking water systems and food chain (Qiao et al., 2018). A primary source of antibiotics and ARGs in aquatic environment originates from effluents discharged from WWTPs (O'Flynn et al., 2021). Therefore, the advanced treatment of trace antibiotics in effluents of WWTPs is of great importance.

To the best of our knowledge, previous studies such as those based on physical adsorption and advanced oxidation processes can efficiently remove antibiotics from secondary effluent of municipal wastewater, but the implementation of these processes may not be feasible due to economic and environmental issues (Xu et al., 2018; Reis et al., 2014). Biodegradation overcomes the problems of high operation costs and secondary pollution (Zhang et al., 2021). However, the removal of antibiotics via biological processes could be inhibited by its bacteriostatic and fungistatic properties, resulting in poor degradation efficiency and long operating time (Zhao et al., 2020). Many efforts have been made to improve the biodegradation efficiency of antibiotics by adding promising additives to improve the metabolic activity of bacteria, and combining biotransformation with other technologies, such as membrane bioreactor (Huang et al., 2019; Do and Stuckey, 2019). But problems such as the massive consumption of additives and membrane fouling get in the way of the development of sustainable wastewater treatment technologies. The extraction of electrons from microorganisms, which belongs to microbial electrochemical technology, has been proposed as a more effective and sustainable bioaugmentation technology that can continuously extract electrons from microbe to accelerate electron transfer, and the biodegradation efficiency of organic contaminants was therefore facilitated by the enhanced microbial oxidation and reduction (Zhou et al., 2020; Yang et al., 2020). Efficient bioremediation of many refractory pollutants with biotoxicity (e.g., chlorinated organic compounds, polycyclic aromatic hydrocarbons, nitrobenzene, and azo dyes, etc.) under electrical stimulation have been reported in the past studies (Kong et al., 2014; Wang et al., 2022; Chen et al., 2019; Wang et al., 2015), overcoming the limitations of poor biodegradation efficiency with low energy and chemical consumption. However, the antibiotic removal by microbial electrochemical technology has so far been mainly explored in the microbial fuel cells and microbial electrolysis cells, which were limited in practical applications due to the complexity in reactor construction and the need for expensive ion exchange membranes or specific electrolytes (Langbehn et al., 2021; Sun et al., 2019).

The accelerated degradation of organic pollutants by the extraction of electrons is accomplished by electroactive biofilms (EABs) formed by exoelectrogens (Logan et al., 2019). Previous studies have mainly focused on optimizing the biodegradation capabilities of EABs by setting different anode potentials and adjusting the dosage of external carbon supply, while the role of the most important basic components of EABs—extracellular polymeric substances (EPS) was neglected (Hou et al., 2019; Hou et al., 2021). EPS, rather than microbial cells, which

accounted for most of the biomass in EABs, play critical roles in the functions and electrochemical properties of EABs (Flemming et al., 2016; Karygianni et al., 2020; Yang et al., 2019; Tan et al., 2019). Attempts have been made to elucidate the effects of EPS composition and spatial distribution on extracellular electron transfer (EET) during electron extraction (Xiao et al., 2017; Li et al., 2020), but the functions of EPS in the biodegradation capabilities of EABs have not yet been adequately elucidated. This could be the first study to optimize biodegradation of organic contaminants by regulating EPS composition. Besides, as one of the most important metabolites secreted by microorganisms (mainly bacteria), EPS are similar in composition to dissolved organic matters (DOM) ubiquitous in both terrestrial and aqueous environments (Zhou et al., 2021). Many studies have confirmed that DOM, which mainly consist of proteins, polysaccharides and humic substances, can produce a variety of reactive species (e.g., triplet excited-states species ($^3\text{DOM}^*$), hydroxyl radical ($\cdot\text{OH}$), singlet oxygen ($^1\text{O}_2$) and superoxide ($\cdot\text{O}_2^-$) under solar irradiation which accounts for the indirect photolysis of antibiotics in natural and engineered aquatic systems (Sharpless, 2012; Yang et al., 2018; Mangalgiri and Blaney, 2017; Maizel and Remucal, 2017). This is one of the most important and least understood sets of photochemical pathways involves in the breakdown of organic contaminants in surface waters (McNeill and Canonica, 2016). However, to the best of our knowledge, this pathway has not been appreciated in wastewater treatment systems.

Based on the above discussion, a sustainably green strategy for the advanced treatment of secondary effluent organic matters (EfOM) was proposed in this study. Sulfadiazine (SDZ), which could be frequently detected in aquatic environments and was considered as one of the “high priority” antibiotics, was chosen as the model high-risk organic contaminants (Hu et al., 2018; Wang et al., 2018). *Rhodospseudomonas palustris* (*R. palustris*), a purple anoxygenic photosynthetic bacteria with good tolerance and degradability to toxic chemicals and refractory pollutants was used as the model microbe (Wu et al., 2019; Getha et al., 1998). Firstly, photosynthetic bacteria were integrated with electrochemical methods as a bioaugmentation technology to accelerate the removal of SDZ from aqueous solution. The continuous extraction of photosynthetic electrons driven by four different external potentials (i.e., -0.2 , 0 , 0.2 , and 0.4 V vs SCE) was employed to regulate the secretion and structure of EPS. Subsequently, EPS secreted by photoheterotrophic metabolism were extracted as a sustainable biomaterial and further used for the indirect photodegradation of SDZ. The response of EPS composition and spatial structure to photosynthetic electron extraction driven by different external potentials and its effect on the biodegradation and indirect photodegradation of SDZ were investigated for the first time to optimize SDZ removal. Additionally, the photosensitive components in EPS and the possible mechanisms for enhanced photodegradation were discussed.

2. Materials and methods

2.1. Experimental setup and operation

The single-chamber electrochemical reactor was constructed by a 140 ml cylindrical glass container with a teflon lid, where graphite plate ($3.0 \times 1.5 \times 0.5$ cm), spring-shaped titanium wire (0.06 cm diameter), and saturated calomel electrode (SCE) were used as working electrode, counter electrode and reference electrode, respectively. The reference electrode was maintained in the middle of the device, and the working and counter electrodes were placed parallel and symmetrically on both sides of it (Fig. S1a). Silica gel ring and B-7000 glue were used to keep the reactor sealed.

R. palustris in the logarithmic growth phase, purchased from Guangdong Microbial Culture Collection Center, were added to the reactors as inoculums and the external potentials of the working electrodes were set to -0.2 , 0 , 0.2 , 0.4 V vs. SCE by a multichannel potentiostat (CHI 1000 C, Chenhua Co. Ltd, Shanghai, China) to acclimatize the *R. palustris* to

form photoelectroactive biofilms (PEABs) on the working electrodes. The culture medium contained CH_3COONa (2 g/L), $\text{K}_2\text{HPO}_4 \cdot 3 \text{H}_2\text{O}$ (7.76 g/L), KH_2PO_4 (2.53 g/L), ferric citrate (0.006 g/L), citric acid (0.006 g/L), EDTA-Na_2 (0.001 g/L), NH_4Cl (0.31 g/L), KCl (0.13 g/L), trace metal solution (12.5 ml/L), and vitamin solution (12.5 ml/L) (Sun et al., 2015). The culture mediums used for the cultivation were sterilized and all inoculation procedures were strictly aseptic. The reactors were run in duplicates in a constant temperature incubator (28 ± 1 °C) and illuminated by a full-spectrum lamp (8000 lux) during the whole experimental process unless otherwise stated.

2.2. SDZ degradation tests

SDZ ($\geq 99\%$ purity) purchased from Sigma-Aldrich (St. Louis, MO, USA) was dissolved in ultrapure water and added to the culture medium through a sterilized $0.22 \mu\text{m}$ microporous filter to reach a final concentration of 1 mg/L. The SDZ biodegradation tests by PEABs with working electrode poised at four different potentials began with the formation of the mature PEABs (Fig. S1b). In order to investigate the contribution of PEABs and photosynthetic electron extraction to SDZ degradation, the reactors were operated repeatedly with abiotic and open-circuit controls. The biodegradation capabilities of PEABs in absolute darkness were also investigated.

After biodegradation tests, the PEABs were scraped off with cell scrapers and the EPS were extracted as a biomaterial to induce the indirect photodegradation of SDZ. All tests related to EPS-induced photodegradation were conducted in sterilized NaCl solution (0.9%) with strictly aseptic operations to avoid microbial degradation. The TOC values of EPS solutions were determined by a Shimadzu TOC-L CPH analyzer (Shimadzu, Kyoto, Japan) and the EPS concentrations used for photodegradation tests were set to 10 and 20 mg/L. Batch experiments were carried out with or without working electrode poised at 0.2 V, an optimal potential for SDZ biodegradation, to explore the influence of external potential. Dark controls were performed to ascertain the photosensitivity and adsorbability of EPS. The $\cdot\text{OH}$ and $^1\text{O}_2$ after 30 min of light irradiation were measured using an electron paramagnetic resonance spectrometer (EPR, EMXplus, Bruker). To explore the contribution of different reactive species in the indirect photodegradation of SDZ induced by EPS, sorbic acid (SA, $>99\%$ purity), isopropanol (IPA, HPLC grade) and furfuryl alcohol (FFA, $>98\%$ purity) were added at concentrations of 200 μM , 100 mM, and 40 μM , respectively, to selectively quench $^3\text{EPS}^*$, $\cdot\text{OH}$ and $^1\text{O}_2$.

2.3. Analytical methods

2.3.1. Chemical analysis

The concentrations of SDZ were determined using high performance liquid chromatography (HPLC, Essentia LC-16; Shimadzu, Osaka, Japan) equipped with a UV detector at 265 nm. The mobile phase consisted of 20:80 (v:v) acetonitrile and 0.5% formic acid were both HPLC grade and purchased from Aladdin Industrial Corporation (Shanghai, China). The separation of SDZ in samples was achieved by a C18 column ($5 \mu\text{m}$; 4.6×150 mm, Phenomenex, CA, USA) with a flow rate of 1 ml/min at 35 °C. The concentrations of CH_3COONa were determined using a method from (Sun et al., 2020).

The intermediate products of SDZ were identified by Ultra performance liquid chromatography Q-Exactive Orbitrap mass spectrometry (UPLC-Q-Orbitrap MS, Thermo Fisher Scientific, CA, USA). A Hypersil GOLD C18 column ($1.9 \mu\text{m}$; 100×2.1 mm, Thermo, MA, USA) was used with the mobile phase consisted of 0.1% formic acid (A) and acetonitrile (B) at a flow rate of 0.25 ml/min. The gradient elution started with 98% A for 2 min, then linearly decreased to 5% in 13 min and kept for 3 min, and finally returned to 98% in 2 min. Samples were analyzed in both negative and positive modes of electrospray ionization (ESI) (m/z 50–750) with a capillary temperature of 320 °C.

The high-resolution mass spectrometry data were obtained using

Compound Discoverer 2.0 (Thermo Scientific), following a method from (Luo et al., 2020). In brief, peak detection and alignment were obtained with the following settings: S/N threshold, 5; mass tolerance, 50 ppm; maximum retention time shift, 0.5 min; and minimum peak intensity, 1×10^4 . The exacted masses were searched in ChemSpider and the MS/MS fragments were compared in the m/z Cloud database.

2.3.2. Electrochemical analysis of PEABs

The electrical signal transformed by the extraction of photosynthetic electrons from the PEABs was recorded every 5 min using a multi-channel potentiostat mentioned above. The electrochemical activity of PEABs was characterized by cyclic voltammetry (CV) measured by an electrochemical workstation (CHI660D, Chenhua Co. Ltd, Shanghai, China), which was performed at a potential range of -0.6 – 0.5 V with a scan rate of 5 mV/s (Sun et al., 2020).

2.4. Extraction, quantification and characterization of EPS

The EPS secreted by *R.palustris* under different operating conditions were extracted using a modified heating protocol (Dai et al., 2016). The PEAB was first scraped into a centrifuge tube using a sterile brush, then the sterile brush was washed a few times to peel off the residual PEAB using 5 ml of 0.9% NaCl solution, and the suspension was further diluted with 5 ml of 0.9% NaCl solution that was preheated to 70 °C to reach an immediate warm temperature of 35 °C. The suspension was sheared by a vortex mixer for 2 min immediately, followed by centrifugation at 5000 g for 15 min. The supernatant was filtered through $0.22 \mu\text{m}$ membrane filter, and the organic matter collected in the supernatant was regarded as the loosely bound EPS (LB-EPS). The bacterial precipitates left in the centrifuge tube were resuspended in 5 ml 0.9% NaCl solution. The suspension was then heated in a water bath for 30 min at 40 °C, centrifuged at 5000 g for 20 min and washed two times using 5 ml of 0.9% NaCl solution. The collected 10 ml supernatant filtered through a $0.22 \mu\text{m}$ membrane filter was regarded as the tightly bound EPS (TB-EPS).

The contents of polysaccharides, proteins and humic acid in EPS were measured using the anthrone-sulfuric acid method (Larsson and Tornkvist, 1996), a BCA Protein Assay Kit (Thermo Scientific Pierce) and a modified Lowry method (Frolund et al., 1995), respectively.

Afterwards, the three-dimensional excitation-emission matrix (3D-EEM) spectra of both LB-EPS and TB-EPS were analyzed to qualitatively and semi-quantitatively determine the fluorescence constituents in EPS using a luminescence spectrometer (FLS1000, Edinburgh Co., UK) with ultrapure water as blank (Xu et al., 2013). The excitation wavelength (Ex) was scanned from 220 to 500 nm with an increment of 5 nm by varying the emission wavelength (Em) from 250 to 700 nm at 5 nm increments. The 3D-EEM data were processed using Matlab (version R2016a) software.

2.5. The spatial distribution of EPS in biofilms

At the end of the experiments, the biofilms were stained directly, and the staining steps were detailed in the Supporting Information (SI-1). Confocal laser scanning microscopy (CLSM, LSM 800 With Airyscan, Carl Zeiss, Germany) was used to visualize the spatial distribution of proteins, α -polysaccharides, β -polysaccharides in the stained biofilms. Randomly sampled view fields were observed and analyzed. Image stacks were obtained using a $5 \times$ objective. Simulated 3D images and sections (plan views) of biofilms were generated under the "Stack" model and analyzed using the software ZEN (Blue Edition, Carl Zeiss).

3. Results and discussion

3.1. Enhanced biodegradation of SDZ by photosynthetic electron extraction

The biodegradation capabilities of PEABs acclimatized at four different external potentials and the enhancement of SDZ biodegradation by photosynthetic electron extraction were investigated. As shown in Fig. 1a, significant removal ratios were observed in all applied-potential groups, with the 58 h removal ratios of SDZ calculated as 66.7%, 74.2%, 78.0%, 69.6% under external potentials of -0.2 , 0 , 0.2 , 0.4 V, respectively. However, in the traditional anaerobic biodegradation system, the operating time required to achieve the same biodegradation ratios obtained in this paper needs to be measured in weeks or even in months (Cheng et al., 2021; Zhao et al., 2022; Wang et al., 2021; Cheng et al., 2021). Besides, the degradation rates of SDZ in reactors operated in open-circuit mode decreased obviously, with a calculated removal ratio of 40.0%. And the pseudo-second-order kinetic rate constant (k) for SDZ obtained at an external potential of 0.2 V was 4.87-folds higher than that in open-circuit mode, indicating that the efficient biodegradation of SDZ could be achieved by the continuous extraction of photosynthetic electrons at 0.2 V. To ascertain the role of photoheterotrophic metabolism in SDZ removal, the biodegradation capabilities of PEABs under the condition of total darkness with external potentials poised at 0.2 V were also tested. Results showed that only 7.7% of SDZ was removed, and the degradation rate constant was less than 0.002 (Fig. 1b). We also found that the utilization rates of CH_3COONa were less than 7% in the dark controls, and no significant current was generated (Fig. 1c-d), which indicated that PEABs formed by *R.palustris* could not use CH_3COONa as carbon source to generate photosynthetic current under dark conditions. These results suggested that the biodegradation capabilities of PEABs could be significantly

enhanced by the extraction of photosynthetic electrons under photoheterotrophic growth, and 0.2 V was the optimal external potential for *R.palustris* to biodegrade SDZ. Setting external potentials which provides continuous electron acceptors to accelerate microbial metabolism may be the underlying mechanisms for the enhanced biodegradation efficiency.

In addition, to testify the contribution of biodegradation by PEABs in the removal of SDZ, the degradation kinetics of SDZ were examined in abiotic controls (Fig. 1b). During 58 h of degradation, SDZ could hardly be removed by photolysis, hydrolysis and electrolysis, and the removal ratios were less than 3%. Therefore, it is evident that the removal of SDZ was microbially mediated, and the extraction of photosynthetic electrons played a critical role in SDZ biodegradation.

The current curves reflected the transfer of photosynthetic electrons produced by PEABs to the working electrodes. A previous study observed that the maximum current decreased with the more positive anode potentials in EABs formed by *Geobacter sulfurreducens* (Scarabotti et al., 2021). The same results were obtained in PEABs inoculated with *R.palustris*, where the PEABs acclimatized at -0.2 and 0.4 V had the highest and lowest maximum current, respectively (Fig. 1d). Combined with the removal ratios of SDZ, it can be seen that the biodegradation capabilities of PEABs had no correlation with the maximum currents but are positively related to the utilization rates of CH_3COONa ($R^2 = 0.993$; $P > 0.05$) (Fig. S2a), which indicated that co-metabolism of CH_3COONa was one of the reasons affecting the biodegradation rates of SDZ. Besides, the photosynthetic current cycles and the utilization rates of CH_3COONa obtained at 0.2 V were the fastest, confirming that the extraction of photosynthetic electrons at an external potential of 0.2 V significantly enhanced the photoheterotrophic metabolism of *R.palustris* with CH_3COONa as carbon source.

The CV scans further illustrated the influence of electrochemical activities of PEABs on SDZ biodegradation. Similar current responses

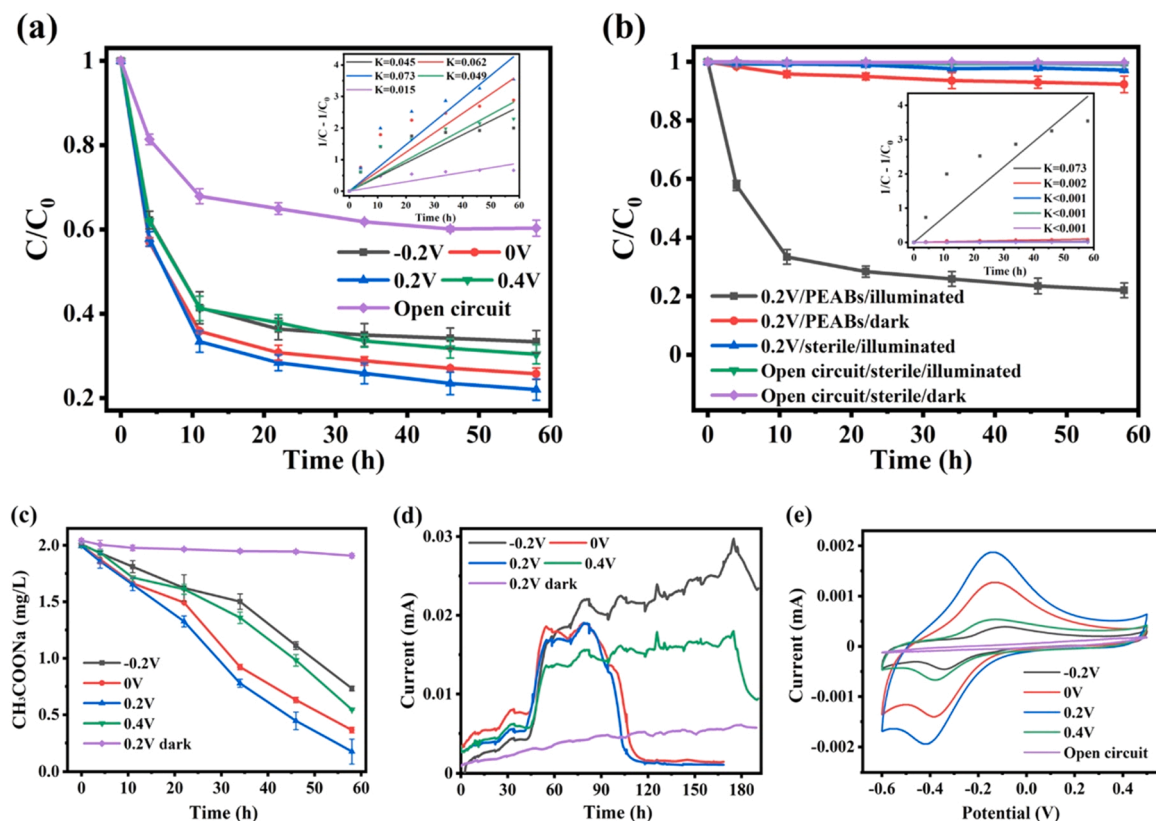


Fig. 1. Removal ratios and kinetics of SDZ under different external potentials (a) and in abiotic and dark controls (b); CH_3COONa utilization rates (c), currents generation (d), and CV scans (e) of PEABs under different external potentials.

were observed under the turnover condition with reduction peaks ranging from -0.34 to -0.41 V and oxidation peaks ranging from -0.08 to -0.14 V (Fig. 1e), suggesting that the electron transfer in PEABs formed by *R. palustris* might be mediated by the same proteins (Li et al., 2017). The calculated mid-point potential around 0.24 V matched the outer membrane cytochromes that has been reported previously (Kim et al., 2002). However, photosynthetic biofilms cultivated in open-circuit mode did not possess such redox peaks, indicating that the extraction of photosynthetic electron altered the extracellular electron transport pathways, promoted the secretion of outer membrane cytochromes, and thus accelerated the SDZ biodegradation rates. The presence of outer membrane cytochromes makes it possible for PEABs to transfer electrons directly by contact (Myers and Myers, 1992). Besides, larger area in the CV curves shows better electrochemical activities of the PEABs (Li et al., 2021), and the peak currents of oxidation peaks obtained in the CV scans were positively related to the degradation rate constants of SDZ under four different external potentials ($R^2 = 0.998$; $P < 0.05$) (Fig. S2b). It follows that the biodegradation capabilities of PEABs were significantly affected by their electrochemical activities. The best electrochemical activities of PEABs acclimatized at 0.2 V benefitted the photoheterotrophic metabolism driven by extraction of photosynthetic electrons, which resulted in the fastest degradation rates of SDZ. This phenomenon is in agreement with a previous study, where EABs grown at 0.2 V exhibited higher catalytic activities than those at other potentials ranging from -0.1 – 0.6 V (Li et al., 2017). These results further confirmed that 0.2 V was the optimal external potential for *R. palustris* to form highly electrocatalytic biofilms and to achieve efficient removal of SDZ by bioaugmentation.

Furthermore, the biodegradation pathways of SDZ by PEABs were proposed in Fig. 2. Totally eleven possible metabolites were speculated based on the detected m/z and deuterated fragment ions in the mass spectrum. Table 1 summarized the proposed structure, formula, retention time and m/z of the intermediate products.

As previously reported, SDZ could be hydrolyzed to form 2-aminopyrimidine (not detected) and sulfanilic acid (M1, $m/z = 174$) by the cleavage of sulfonamide bond. Among them, M1 could be reduced to 4-aminobenzoic acid (M2, $m/z = 158$) under anaerobic denitrification conditions or converted to 4-hydroxybenzenesulfonic acid (not detected) under anaerobic conditions. 4-hydroxybenzenesulfonic acid was further converted to 3,4-dihydroxybenzenesulfonic acid (M3, $m/z = 191$), then, 1,2,4-benzenetriol (M4, $m/z = 127$) was produced by bioconversion of 4-hydroxybenzenesulfonic acid and M3 (Zhang et al., 2021; Xie et al., 2020). Finally, M5 ($m/z = 159$) was formed from M4 through the cleavage of intradiol ring. Besides, hydroxylation of 2-aminopyrimidine plays a vital role in SDZ biodegradation because the pyrimidine ring is similar in chemical characteristic to the benzene ring which is prone to be hydroxylated (Zheng et al., 2020). Therefore, 2-aminopyrimidine could be transformed to 2,5-dihydroxypyrimidine (M6, $m/z = 113$) and isocytosine (M7, $m/z = 112$) by hydroxylation. Additionally, 4-[2-iminopyr-imidine-1(2H)-yl] aniline (M8, $m/z = 187$) was formed by the reaction between 2-aminopyrimidine and M1, and N-[4-(Hydroxyamino)phenyl]-2-pyridinamine (M9, $m/z = 203$) was derived from the reaction between 2-aminopyrimidine with N-aryl-hydroxylamine, formed from the oxidation of aniline, where aniline was originated from the M1 (Teng et al., 2020; de Amorim et al., 2014). In addition to the hydrolysis pathways, two direct transformations of SDZ have been reported in previous studies. The first transformation was that the SO_2 on SDZ was extruded to form N-(2-Pyrimidinyl)-1,4-benzenediamine (M10, $m/z = 187$), and the second one was the hydroxylation of SDZ to form 5-OH-sulfadiazine (M11, $m/z = 267$) (Zheng et al., 2020; Chen et al., 2021).

z = 191), then, 1,2,4-benzenetriol (M4, $m/z = 127$) was produced by bioconversion of 4-hydroxybenzenesulfonic acid and M3 (Zhang et al., 2021; Xie et al., 2020). Finally, M5 ($m/z = 159$) was formed from M4 through the cleavage of intradiol ring. Besides, hydroxylation of 2-aminopyrimidine plays a vital role in SDZ biodegradation because the pyrimidine ring is similar in chemical characteristic to the benzene ring which is prone to be hydroxylated (Zheng et al., 2020). Therefore, 2-aminopyrimidine could be transformed to 2,5-dihydroxypyrimidine (M6, $m/z = 113$) and isocytosine (M7, $m/z = 112$) by hydroxylation. Additionally, 4-[2-iminopyr-imidine-1(2H)-yl] aniline (M8, $m/z = 187$) was formed by the reaction between 2-aminopyrimidine and M1, and N-[4-(Hydroxyamino)phenyl]-2-pyridinamine (M9, $m/z = 203$) was derived from the reaction between 2-aminopyrimidine with N-aryl-hydroxylamine, formed from the oxidation of aniline, where aniline was originated from the M1 (Teng et al., 2020; de Amorim et al., 2014). In addition to the hydrolysis pathways, two direct transformations of SDZ have been reported in previous studies. The first transformation was that the SO_2 on SDZ was extruded to form N-(2-Pyrimidinyl)-1,4-benzenediamine (M10, $m/z = 187$), and the second one was the hydroxylation of SDZ to form 5-OH-sulfadiazine (M11, $m/z = 267$) (Zheng et al., 2020; Chen et al., 2021).

3.2. Indirect photodegradation of SDZ induced by EPS extracted from PEABs

As inevitable metabolites secreted by PEABs, EPS are a significant source of DOM present in natural waters, which contributes to the indirect photodegradation of antibiotics through the generation of excited triplet state EPS ($^3\text{EPS}^*$) and other reactive species in sunlit waters (Zhou et al., 2021; Gong et al., 2012; Ryan et al., 2011). In this study, there could be three possible degradation pathways of SDZ, which includes photoheterotrophic co-metabolic degradation, indirect photodegradation induced by EPS secreted by PEABs, and direct photolysis. Among them, Section 3.1 confirmed that the photoheterotrophic metabolism of *R. palustris* was the main degradation pathway of SDZ, while the direct photolysis of SDZ was negligible. However, the contribution of indirect photodegradation induced by EPS to SDZ removal was unknown. Therefore, a series of experiments in the absence and presence of EPS as well as the corresponding dark controls were conducted to further investigate the role of EPS in PEABs on the indirect

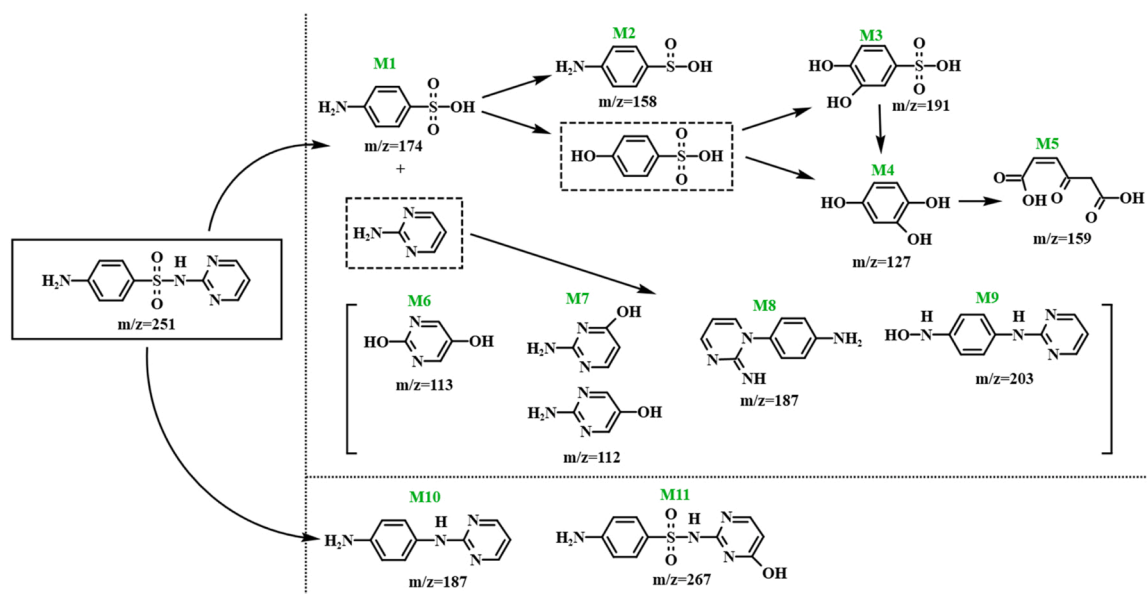
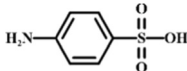
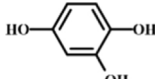
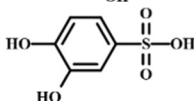
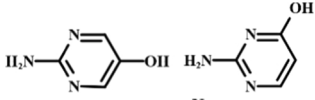
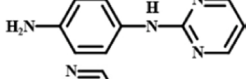
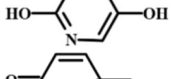
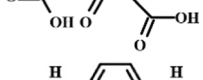
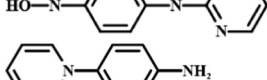
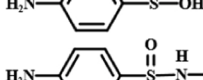
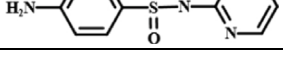


Fig. 2. Proposed degradation pathways of SDZ by PEABs based on detected metabolites (Compounds in the dashed boxes were not detected in this study due to sampling time or low sample concentrations).

Table 1
Summary of the identified degradation products of SDZ.

Substance	Formula	Proposed structure	t _R (min)	m/z
M1	C ₆ H ₇ NO ₃ S		0.224	174.01466
M4	C ₆ H ₆ O ₃		0.76	127.03169
M3	C ₆ H ₆ O ₅ S		0.945	190.99359
M7	C ₄ H ₅ N ₃ O		1.087	112.04326
M10	C ₁₀ H ₁₀ N ₄		1.339	187.09055
M6	C ₄ H ₄ N ₂ O ₂		1.466	113.02728
M5	C ₆ H ₆ O ₅		1.741	159.02152
M9	C ₁₀ H ₁₀ N ₄ O		2.098	203.08546
M8	C ₁₀ H ₁₀ N ₄		5.094	187.09055
M2	C ₆ H ₇ NO ₂ S		5.633	158.01975
M11	C ₁₀ H ₁₀ N ₄ O ₃ S		6.028	267.04736
SDZ	C ₁₀ H ₁₀ N ₄ O ₂ S		6.418	251.05245

photodegradation of SDZ.

As shown in Fig. 3a-b, in the absence of EPS, no obvious degradation was observed under both applied potential of 0.2 V and open circuit conditions. However, the addition of EPS significantly accelerated the photodegradation of SDZ with rate constants increased by 19.5–35.6 times for applied potential groups, and 262.0–584.8 times for open circuit groups. And the photodegradation rates of SDZ induced by EPS extracted from four different PEABs in open-circuit mode were faster than those with external potential poised at 0.2 V. It may be attributed to the competition of electrode for reactive species or the external potential inhibiting the production of reactive species. The inhibition mechanism of applying external potentials on the EPS-induced photodegradation remains to be studied by further research. Additionally, the EPS extracted from PEABs acclimatized at 0.2 V exhibited better photodegradation efficiencies than those acclimatized at -0.2, 0, 0.4 V, which was roughly consistent with the biodegradation results obtained in Section 3.1. This can be interpreted as the PEABs with better electrochemical activities contain more redox active substances (e.g., humic substances and proteins) in EPS, resulting in better photosensitivity (Tenorio et al., 2017).

Besides, SDZ recoveries of more than 99% from the dark controls after 58 h (Fig. 3c) indicated that EPS at the concentration of 20 mg/L had almost no adsorption and degradation effect on SDZ. And the photodegradation rates decreased obviously when the addition of EPS was

reduced to 10 mg/L, which might be related to the decrease in the abundance of photosensitive substances (Lee et al., 2013). Notably, a complete removal of SDZ within 58 h operated in open-circuit mode was observed in presence of the EPS extracted from PEABs acclimatized at 0.2 V, suggesting that EPS accumulated in PEABs has a great potential in the preparation of biomaterials for the high-efficiency removal of residual antibiotics present in effluents discharged from WWTPs. Although the removal efficiency of SDZ induced by EPS is unlikely on a par with that of the advanced treatment technologies commonly used in practical WWTPs, the extracted EPS ameliorates the problems of high costs and secondary pollution caused by the large consumption of energy and chemical reagents since EPS are inevitable products of microbial metabolism and naturally exist in aquatic environment, which could be a promising technology for sustainable wastewater treatment. The lower removal ratios (66.7–78.0% within 58 h) of SDZ obtained in biodegradation tests (Section 3.1) may be attributed to the quenching of reactive species by natural antioxidants, such as carotenoids and enzymes, secreted by *R. palustris* (Ge and Liu, 2020).

Previous studies have confirmed the existence of $\cdot\text{OH}$, $^1\text{O}_2$, and $\text{O}_2\cdot^-$ in the photodegradation of organics induced by photosensitive substances which are similar in composition to EPS (He et al., 2018; Tian et al., 2019; Rosario-Ortiz and Canonica, 2016). Therefore, the EPR technique was applied to characterize the production of reactive species by EPS extracted from PEABs. As shown in Fig. 3d, a relatively strong-OH signal

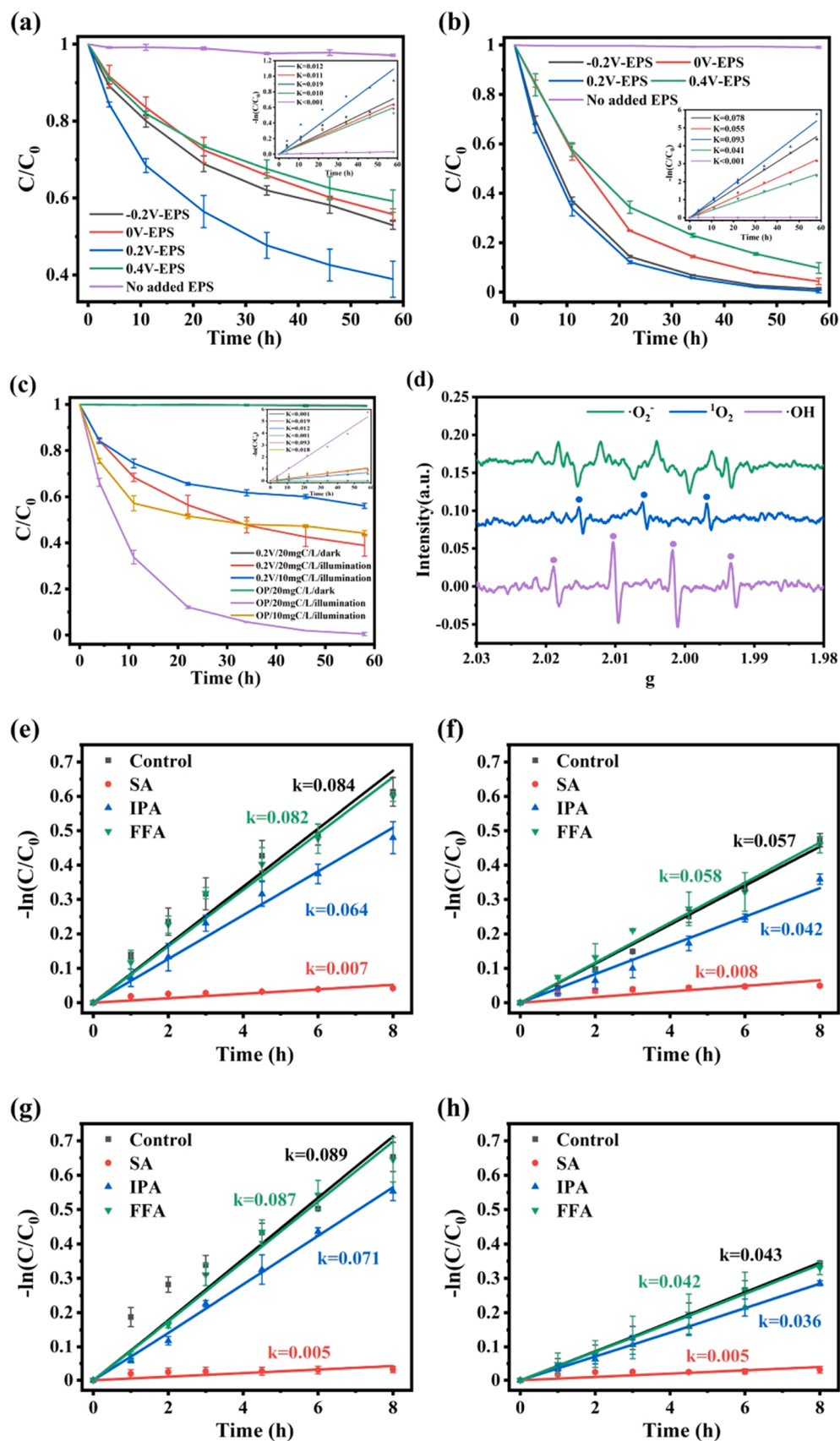


Fig. 3. Photodegradation rates and kinetics of SDZ under applied potential of 0.2 V (a) and open circuit conditions (b) by EPS extracted from PEABs acclimatized at different external potentials; (c) Comparison of photodegradation rates and kinetics of SDZ by EPS extracted from PEABs acclimated at 0.2 V under different operating conditions; (d) EPR spectra of EPS under light irradiation; Photodegradation rates of SDZ by EPS extracted from PEABs acclimatized at - 0.2 V (e), 0 V (f), 0.2 V (g), and 0.4 V (h) in the presence of quenchers.

and a weak $^1\text{O}_2$ signal were observed, while $\cdot\text{O}_2^-$ signal was not detected. To further explore the contributions of different reactive species to the indirect photodegradation of SDZ induced by EPS, $^3\text{EPS}^*$, $\cdot\text{OH}$ and $^1\text{O}_2$ were selectively quenched by scavengers (i.e., SA for $^3\text{EPS}^*$, IPA for $\cdot\text{OH}$, FFA for $^1\text{O}_2$, respectively). The photodegradation rates of SDZ in quenching experiments were compared in Fig. 3d-g. Extremely low photodegradation rates were observed in the presence of SA, when compared to control groups without the addition of quenchers, which was in accordance with the previous studies that EPS could be photoexcited to form $^3\text{EPS}^*$ and predominated in the photodegradation of refractory organic contaminants (Zhang et al., 2019; He et al., 2020). Besides, the addition of IPA reduced the photodegradation rates by 17.7–26.6%, which confirmed the existence of $\cdot\text{OH}$ in the EPS-induced photodegradation of SDZ. The formation of $\cdot\text{OH}$ could be attributed to the humic substances with highly photoreactive chromophores present in EPS, which have been known as a good source to produce $\cdot\text{OH}$ by absorbing light (Lee et al., 2013). At the same time, with dosing of FFA to quench $^1\text{O}_2$, the photodegradation rates of all four groups induced by EPS extracted from PEABs acclimatized at different external potentials stayed almost unchanged, which suggested that $^1\text{O}_2$ was negligible in the indirect photodegradation of SDZ. These results obtained above were generally consistent with previous studies on extracellular organic matters (EOM) secreted by algae, where excited triplet state EOM ($^3\text{EOM}^*$) played a dominant role in the photolysis of antibiotics with the contribution around 90%. However, unlike the EOM-induced photodegradation system, $\cdot\text{OH}$ was generated in this study and played a non-negligible role in the indirect photodegradation of SDZ (Tian et al., 2019; Tian et al., 2019).

It's worth mentioning that the photodegradation of organics is attributed to the reactive species generated under sunlight irradiation, and the yield of reactive species greatly affects the degradation efficiency of target pollutants (McNeill and Canonica, 2016). Metal ions have been reported to complex with DOM to inhibit the formation of $^3\text{DOM}^*$ (Wan et al., 2019), which may greatly reduce the phototransformation of organic pollutants induced by EPS. But another study has reported that high salinity would accelerate the photodegradation of several polycyclic aromatic hydrocarbons (PAHs) in the presence of DOM (Shang et al., 2015). Moreover, Guo et al. (2022) reported that the inhibition effects of DOM and NO_3^- on the photodegradation of two antidepressants which are degraded mainly via direct photolysis in lake water were attributed to the screening effects or quenching effects. However, for citalopram, which attenuates naturally mainly through indirect photolysis, the photodegradation efficiency was significantly enhanced by the addition of DOM and NO_3^- . Therefore, EPS, as a new type of sustainably green biomaterial, will have broad development prospects in the phototransformation of refractory organics which are difficult to achieve naturally attenuation by direct photolysis. It is undeniable that the composition of secondary effluent is rather complex (including a variety of refractory organics, co-existing ions, and particles, etc.), and further studies need to be conducted to elucidate the mechanism of separate and joint effects of different effluent components on the photogeneration of reactive species derived from EPS in the future.

3.3. EPS composition regulated by external potentials

R.palustris adheres to the surface of working electrodes poised at different potentials and develops into PEABs encased in self-produced EPS (Das et al., 2013). The process of photosynthetic electron extraction driven by different external potentials will result in different EPS composition and spatial structure in PEABs. EPS have been demonstrated to be fundamental microbial components that determine the physicochemical properties of biofilms and have multiple environmental functions, one of which is to function as a conductive matrix that transfers electrons by utilizing extracellular protein-like and humic-like substances (Yang et al., 2019; Cai et al., 2018). Previous studies have

confirmed the existence of cytochromes c and flavins in EPS from electroactive bacteria by electrochemical measurements and proteomics technology, and the extracellular proteins in EPS were identified as key redox species for electroactive bacteria (Xiao and Zhao, 2017). However, the relationship between EPS composition and the biodegradation capabilities of EABs was rarely investigated. Besides, EPS can generate reactive species for the photodegradation of organic contaminants under simulated sunlight irradiation, which is critically important in the remediation of aquatic ecosystems and in driving biogeochemical element cycling (Li et al., 2016). A previous study has reported that the production of reactive species varies with the optical properties, molecular weight, and composition of DOM present in natural and engineered aquatic systems (Maizel and Remucal, 2017). Similarly, the compositional differences in EPS extracted from different PEABs will exhibit variable generation of, and reaction with, reactive species during SDZ photodegradation. In these regards, the composition and production of EPS in PEABs regulated by different external potentials were measured, and their effects on biodegradation capabilities of PEABs and indirect photodegradation of SDZ were analyzed.

As shown in Fig. 4, the contents of all analyzed constituents in EPS, including humic acid, proteins, and polysaccharides, could be significantly affected under long-term regulation of different external potentials. EPS extracted from PEABs, also known as bound EPS, are greatly affected by external potentials and can be divided into LB-EPS and TB-EPS with respect to their association states with bacterial cells (Cao et al., 2011). It can be seen that the content of each constituent in TB-EPS is generally higher than that in LB-EPS (Fig. 4a-c). Tightly attached to the cell surface as peripheral capsules, TB-EPS are affected more by the metabolic activities of bacterial cells under the regulation of different external potentials than by the environment (Xiao and Zhao, 2017). The rate constants of SDZ biodegradation were found to be positively related to the contents of proteins in TB-EPS, while had little to do with the contents of humic acid in TB-EPS ($R^2 = 0.723$ and 0.003 for the contents of proteins and humic acid in TB-EPS, respectively; $P < 0.05$) (Fig. S3). This can be interpreted as the biodegradation capabilities of PEABs are significantly affected by their electrochemical activities, which may be mainly dependent on the amounts of redox proteins. Under the long-term regulation of 0 V and 0.2 V, PEABs tended to secrete more extracellular proteins that were tightly bound to cells, which may be related to the higher electrochemical activities of PEABs observed in the CV scans and resulted in better removal ratios of SDZ. In addition, setting external potentials of -0.2 and 0.2 V were beneficial for the secretion of humic acid in TB-EPS, while 0 and 0.4 V promoted the accumulation of polysaccharides in TB-EPS.

The total amounts of EPS in PEABs acclimatized at -0.2 , 0, 0.2 , 0.4 V were 12.04, 13.85, 14.49, 13.16 mg/g dry cell, respectively, while only 10.14 mg/g dry cell of EPS could be produced under open-circuit condition (Fig. 4d), suggesting that the secretion of EPS could be stimulated by photosynthetic electron extraction, and 0.2 V is the optimal potential for the accumulation of EPS in PEABs. Previous studies have demonstrated the presence of numerous adsorption sites and good adsorption capabilities of EPS for sulfonamides (Pi et al., 2019; Wang et al., 2018). Therefore, the increased EPS production may lead to the enrichment of SDZ in PEABs and facilitate their utilization and biodegradation. According to these results, the better removal ratios of SDZ at 0 V and 0.2 V could be partly attributed to the higher production of EPS. Proteins and polysaccharides were measured to be the main constituents of EPS in PEABs formed by *R.palustris*. Compared with the EPS extracted from photosynthetic biofilms cultivated in open-circuit mode, the proportion of proteins increased when external potentials were poised at -0.2 and 0.2 V, while setting external potentials of 0 and 0.4 V increased the proportion of polysaccharides (Fig. 4e). This result was in accordance with the previous finding that the applied potential of 0.4 V was not conducive to the secretion of extracellular proteins but promoted the accumulation of polysaccharides in EPS (Hou et al., 2020). In contrast, the total amounts of humic acid were relatively small with

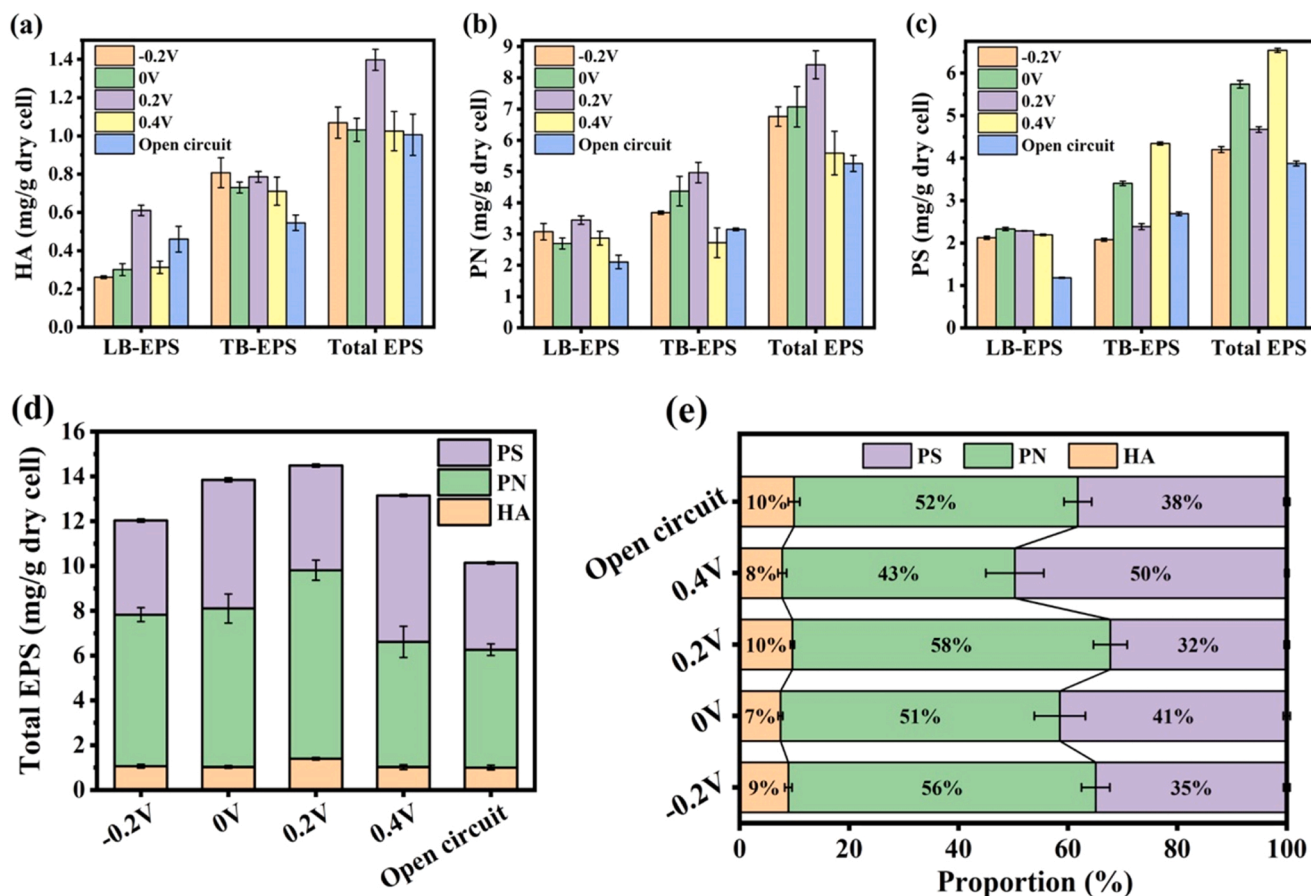


Fig. 4. Contents of humic acid (HA) (a), proteins (PN) (b) and polysaccharides (PS) (c) in LB-EPS, TB-EPS and total EPS extracted from PEABs acclimatized at different external potentials; Stack diagram (d) and scale diagram (e) of each constituent in total EPS.

an average of 1.12 mg/g dry cell. Since the humic fraction in EPS have been demonstrated to have the most significant impact on the formation of $\cdot\text{OH}$ (Lee et al., 2013), the less production of $\cdot\text{OH}$ caused by the low content of humic acid in EPS may be the reason for the minor contribution of $\cdot\text{OH}$ to the SDZ photodegradation. Besides, previous studies have reported that electron transfer in EABs can be mediated by extracellular redox-active proteins and humic substances (Kumar et al., 2017). Therefore, the lower secretion of proteins and humic acid may be one of the reasons for the lower photosynthetic currents obtained in the PEABs acclimatized at 0.4 V.

In addition, the photodegradation rates of SDZ induced by different EPS obtained in Section 3.2 were found to be positively correlated to the total amounts of proteins and humic acid ($R^2 = 0.863$ and 0.870 for applied potential and open circuit conditions, respectively; $P < 0.05$) (Fig. S4), which indicated that the extracellular proteins and humic acid accumulated in PEABs might have the same photosensitive properties as DOM in sunlit waters. The relatively low correlations might indicate the presence of proteins that didn't participate in the photodegradation of SDZ, and the presence of other photosensitive substances, such as fulvic acids.

3.4. 3D-EEM fluorescence spectra of EPS

3D-EEM technology has been widely used to identify soluble organic compounds in EPS, especially protein-like substances and humic substances, based on their basic fluorescence properties (Xu et al., 2020). The aromatic structures and unsaturated aliphatic hydrocarbons in organic matters are the main factors to generate fluorescence (Baker, 2002). The 3D-EEM fluorescence spectra of LB-EPS and TB-EPS extracted from PEABs acclimatized at different external potentials as well as

open circuit controls were illustrated in Fig. 5. The detailed peak locations and fluorescence intensities were summarized in Table S2. It is obvious that EPS extracted from different PEABs had similar fluorescence peaks with different fluorescence intensities. Results showed that five and seven main constituents were identified in LB-EPS and TB-EPS, respectively. Peak A (Ex/Em of 275–280/325–350 nm), peak B (Ex/Em of 230–235/285–315 nm), and peak C (Ex/Em of 230–235/285–315 nm) were all protein-like substances, representing tryptophan, tyrosine, and tryptophan protein-like substances, respectively (Sheng and Yu, 2006). Peak D (Ex/Em of 265–275/445–465 nm) and peak F (Ex/Em of 275–280/500–515 nm) were corresponded to the peaks of fulvic acid-like substances. Peak E (Ex/Em of 345–370/450–465 nm) and peak G (Ex/Em of 365–370/520–530 nm) were assigned to humic acid-like substances (Chen et al., 2003). Fulvic acid-like and humic acid-like substances are both humic substances. The fluorescence intensities of peak A, peak B and peak C in both LB-EPS and TB-EPS enhanced under the regulation of external potentials compared with that in open-circuit mode, especially for those extracted from 0.2 and -0.2 V, indicating that photosynthetic electron extraction significantly stimulated the production of protein-like substances in bound EPS. However, expect for 0.2 V, the fluorescence intensities of peak D and peak E increased in TB-EPS, while decreased slightly in LB-EPS after the regulation of external applied potentials. In addition, slightly decrease occurred in the fluorescence intensities of peaks F and peak G in TB-EPS compared with the open-circuit groups. Overall, the secretion of humic substances could be slightly enhanced by photosynthetic electron extraction, which was consistent with the composition analysis of EPS obtained in Section 3.3.

Previous studies have reported that tryptophan, tyrosine, humic acid and fulvic acid, when irradiated, can produce reactive species in

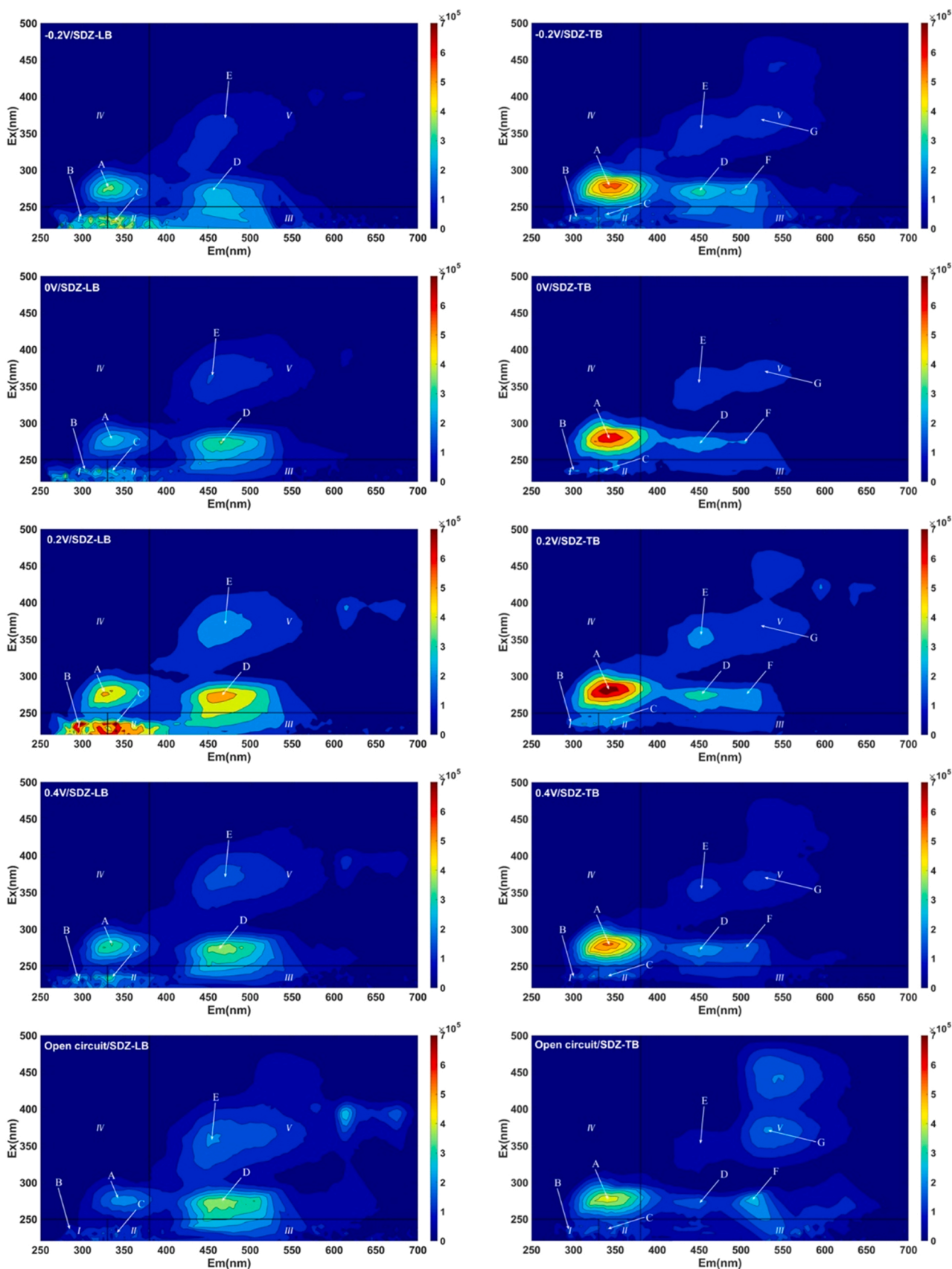


Fig. 5. Three-dimensional EEM (3D-EEM) spectra of LB-EPS and TB-EPS extracted from PEABs acclimatized at different anode potentials.

aqueous solution to induce the photodegradation of organic pollutants (Korytowski et al., 1987; Igarashi et al., 2007). Therefore, the correlations between photodegradation rates of SDZ induced by EPS and the corresponding fluorescence intensities of four main constituents detected in 3D-EEM fluorescence spectra were investigated. As shown in Fig. 6, tryptophan protein-like, tyrosine protein-like, humic acid-like and fulvic acid-like substances in EPS showed significantly positive linearity with the photodegradation rate constants induced by EPS operated at an external potential of 0.2 V ($R^2 = 0.993, 0.971, 0.933$ and 0.981 for tryptophan protein-like, tyrosine protein-like, humic acid-like and fulvic acid-like substances, respectively; $P < 0.05$), while were weakly correlated with that in the open-circuit groups ($R^2 = 0.677, 0.883, 0.543$ and 0.629 for tryptophan protein-like, tyrosine protein-like, humic acid-like and fulvic acid-like substances, respectively; $P < 0.05$). This result confirmed that the increase in the accumulation of photosensitive substances (i.e., protein-like substances and humic substances) in EPS was responsible for the accelerated photodegradation of SDZ. Besides, previous studies have reported that carbonyl-containing compounds in DOM are susceptible to be excited due to the low energy required for electronic transition, which could be responsible for the formation of reactive species including excited triplet states (McNeill and Canonica, 2016; Tian et al., 2019). The locations of peak B in both LB-EPS and TB-EPS extracted from PEABs were red shifted to longer wavelengths compared with those extracted from the photosynthetic biofilms cultivated in open-circuit mode, indicating the increase of some functional groups, such as carbonyl, amino and carboxyl groups, which further confirmed the promotion of photosynthetic electron extraction on the secretion of photosensitive substances (Tian et al., 2019).

3.5. CLSM visualization of EPS in the *R.palustris* biofilms

The presence of EPS preliminarily enhanced the contacts of bacterial cells to its attached surface, which was favorable for interface reactions. The electron transfer capability of EAB across the EPS layer to the electrode depends mainly on the spatial distribution of specific proteins and electron shuttles (Gao et al., 2019). To further investigate the differences in the spatial structure of EPS accumulated at different external potentials and elucidate the effect of the spatial distribution of two main constituents (polysaccharides and proteins) in EPS on the electrochemical properties and biodegradation capabilities of PEABs, the fluorescence in situ hybridization images of the stained biofilms were visualized.

As shown in Fig. 7, proteins and α -polysaccharides were homogeneously distributed in the outer and inner layers of EPS in sheets, respectively, while β -polysaccharides were scattered in the whole EPS in the form of dots. The thicknesses of stained PEABs followed the order of $0.2\text{ V} > 0.4\text{ V} > -0.2\text{ V} > 0\text{ V}$, with a maximum thickness of $235\ \mu\text{m}$ obtained at 0.2 V , while the biofilms formed in open-circuit mode were thinner with an average thickness of $116.5\ \mu\text{m}$. This result further confirmed that photosynthetic electrons extraction stimulated the secretion of EPS and promoted the formation of biofilms, and the external potential of 0.2 V significantly increased the rate of biofilm accumulation. A previous study observed that the current generated by EABs decreased with the increase of biofilm thickness (Sun et al., 2016), which explains why the maximum currents generated at 0.2 and 0.4 V were relatively low. Besides, the average fluorescence intensities of each constituent were compared in Fig. S5. Except for the PEAB acclimatized at 0 V , the average fluorescence intensities of proteins had strongly correlation with the biodegradation rate constants obtained Section 3.1 ($R^2 = 0.984$ and 0.488 for linear fittings excluding and including 0 V , respectively; $P < 0.05$) (Fig. S6), suggesting that the PEABs with higher fluorescence intensities of extracellular proteins possessed better biodegradation capabilities. Although the lowest average fluorescence intensities of proteins were obtained at 0 V , the fluorescence intensities of α -polysaccharides were much higher. A previous study has reported

that the increased secretion of extracellular polysaccharides greatly improved the cell viability of the inner biofilm, which was conducive to reduce the electron transfer resistance of the biofilm (Zhuang et al., 2020). Therefore, the relatively high electrochemical activities and biodegradation capabilities of PEABs acclimatized at 0 V may be related to the higher cell viability in the inner layer and the thinner thickness of PEABs. Besides, β -polysaccharides have been confirmed to be the backbone of a network-like outer layer to maintain the structural stability of the aerobic granule (Adav et al., 2008), therefore, the β -polysaccharides scattered in EPS in dots may play a very important role in maintaining the stability of PEABs. The average fluorescence intensities of β -polysaccharides at 0.2 V were 2.4–3.9 times higher than that observed at the other external potentials, which further demonstrated that 0.2 V was the optimal external potential for *R.palustris* to form stable PEABs with the highest electrochemical activity and best biodegradation capability towards SDZ.

To further illustrate the electron transfer between exogenous electrodes and PEABs, the stained biofilms could be divided into two layers concerning the difference in contact interfaces. The outer layer was in direct contact with the culture medium for substance exchange with the components in the culture medium, while the inner layer was close to the electrode-biofilm interface for electron transfer with the exogenous solid-phase electron acceptor. And the proportion of each constituent in outer and inner layers of PEABs were calculated in Table S3. It can be visually seen from Fig. 7 that α -polysaccharides were distributed at the bottom of the stained biofilms, closest to the electrode side, which may have a nonnegligible impact on the electron transfer between PEABs and the graphite plates. As previously reported, non-conductive polysaccharides can interfere with the electron transfer between redox active proteins on the outer membrane and the electrode (Kouzuma et al., 2010). In PEABs inoculated with *R.palustris*, a strongly negative correlation ($R^2 = 0.993$; $P < 0.05$) was found between the maximum currents produced at different external potentials and the proportion of α -polysaccharides in the inner layers (Fig. S6), which further confirmed the disturbance of α -polysaccharides distributed near the electrode side on the photosynthetic electron transfer from photosynthetic bacteria to the solid electrode. Therefore, higher proportion of α -polysaccharides in the inner layer accumulated at 0.4 V strongly affected the transfer of electrons to the electrode, exerting a negative influence on current generation. The result was consistent with a previous study that relatively high anode potentials promoted the accumulation of polysaccharides in the interior biofilm layers formed by *Geobacter soli*, which might be the direct cause for low current generation (Yang et al., 2019).

4. Conclusion

As one of the most important bacterial metabolites, EPS played a nonnegligible role in affecting biodegradation capabilities of PEABs and indirect photodegradation efficiency of SDZ. The bioaugmentation driven by photosynthetic electron extraction significantly accelerated the biodegradation of SDZ with low energy and chemical consumption. The enhanced SDZ removal ratios were closely related to the electrochemical activities of PEABs which was attributed to the extracellular proteins abundant in EPS. Additionally, this study demonstrates for the first time that EPS, as a renewable and green biomaterial, regulated by different external potentials during the extraction of photosynthetic electrons had a considerable impact on the indirect photodegradation rates of SDZ. Among them, EPS extracted from PEABs acclimatized at 0.2 V exhibited the highest photodegradation rate of SDZ with a complete removal within 58 h. The tryptophan protein-like, tyrosine protein-like, humic acid-like and fulvic acid-like substances present in EPS inoculated with *R.palustris* might be the main effective components which is photosensitive. Furthermore, the contributions of three possible reactive species to the indirect photodegradation of SDZ induced by EPS extracted from PEABs followed the order ${}^3\text{EPS}^* > \cdot\text{OH} > {}^1\text{O}_2$, where the reaction between ${}^3\text{EPS}^*$ and SDZ accounted for 90% of

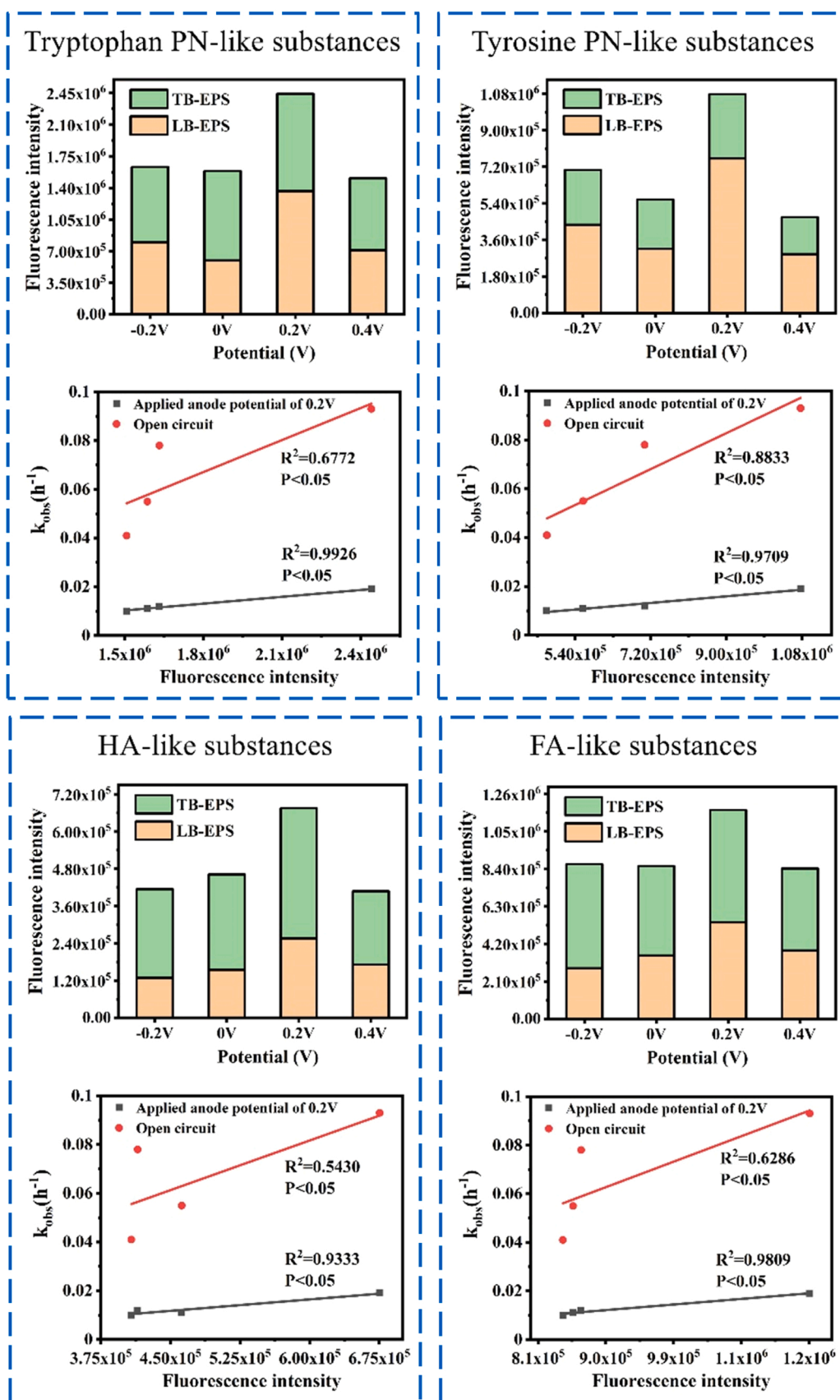


Fig. 6. Fluorescence intensities of four main constituents in EPS extracted from PEABs acclimatized at different external potentials, and their linear relations with corresponding photodegradation rate constants.

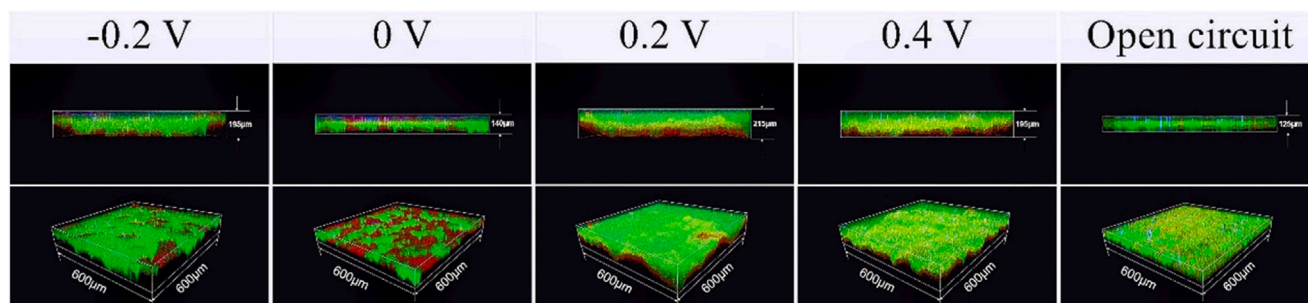


Fig. 7. Spatial distribution of proteins (green), α - polysaccharides (red) and β - polysaccharides (blue) in PEABs acclimatized at different external potentials.

SDZ removal. The excellent removal ratios of SDZ obtained in this study provides a green and sustainable strategy for the removal of high-risk EfOM and brings new inspiration to the exploration of environment-friendly renewable biomaterials.

CRediT authorship contribution statement

Mengmeng Zhao: Conceptualization, Investigation, Writing – original draft. **Xiaoyan Bai:** Investigation. **Yaping Zhang:** Investigation. **Yong Yuan:** Review, Methodology. **Jian Sun:** Conceptualization, Review, Supervision.

Declaration of Competing Interest

The authors declare that they have no known competing financial interests or personal relationships that could have appeared to influence the work reported in this paper.

Acknowledgment

This research was financially supported by the National Natural Science Foundation of China (No. 51108186), Tip-top Scientific and Technical Innovative Youth Talents of Guangdong Special Support Program, China (No. 2015TQ01Z039) and Guangzhou Municipal Science and Technology Project, China (No. 202002030391).

Appendix A. Supporting information

Supplementary data associated with this article can be found in the online version at [doi:10.1016/j.jhazmat.2022.128350](https://doi.org/10.1016/j.jhazmat.2022.128350).

References

- Advav, S.S., Lee, D.-J., Tay, J.-H., 2008. Extracellular polymeric substances and structural stability of aerobic granule. *Water Res.* 42, 1644–1650.
- de Amorim, K.P., Romualdo, L.L., Andrade, L.S., 2014. Performance and kinetic-mechanistic aspects in the electrochemical degradation of sulfadiazine on boron-doped diamond electrode. *J. Braz. Chem. Soc.* 25, 1484–1492.
- Baker, A., 2002. Fluorescence properties of some farm wastes: implications for water quality monitoring. *Water Res.* 36, 189–195.
- Cai, X.X., Huang, L.Y., Yang, G.Q., Wen, J.L., Zhou, S.G., 2018. Transcriptomic, proteomic, and bioelectrochemical characterization of an exoelectrogen geobacter *Soli* grown with different electron acceptors. *Front. Microbiol.* 9 (-).
- Cao, B., Shi, L., Brown, R.N., Xiong, Y., Fredrickson, J.K., Romine, M.F., Marshall, M.J., Lipton, M.S., Beyenal, H., 2011. Extracellular polymeric substances from *Shewanella* sp. HRCR-1 biofilms: characterization by infrared spectroscopy and proteomics. *Environ. Microbiol.* 13, 1018–1031.
- Cheng, D., Huo Hao, N., Guo, W., Chang, S.W., Dinh Duc, N., Quynh Anh, N., Zhang, J., Liang, S., 2021. Improving sulfonamide antibiotics removal from swine wastewater by supplying a new pomelo peel derived biochar in an anaerobic membrane bioreactor. *Bioresour. Technol.* 319.
- Cheng, D., Ngo, H.H., Guo, W., Chang, S.W., Dinh Duc, N., Liu, Y., Liu, Y., Deng, L., Chen, Z., 2021. Evaluation of a continuous flow microbial fuel cell for treating synthetic swine wastewater containing antibiotics. *Sci. Total Environ.* 756.
- Chen, X., Deng, F., Liu, X., Cui, K.-P., Weerasooriya, R., 2021. Hydrothermal synthesis of MnO₂/Fe(0) composites from Li-ion battery cathodes for destructing sulfadiazine by photo-Fenton process. *Sci. Total Environ.* 774.

- Chen, H., Lu, D., Chen, L., Wang, C., Xu, X., Zhu, L., 2019. A study of the coupled bioelectrochemical system-upflow anaerobic sludge blanket for efficient transformation of 2,4-dichloronitrobenzene. *Environ. Sci. Pollut. Res.* 26, 13002–13013.
- Chen, W., Westerhoff, P., Leenheer, J.A., Booksh, K., 2003. Fluorescence excitation - Emission matrix regional integration to quantify spectra for dissolved organic matter. *Environ. Sci. Technol.* 37, 5701–5710.
- Dai, Y.-F., Xiao, Y., Zhang, E.-H., Liu, L.-D., Qiu, L., You, L.-X., Mahadevan, G.D., Chen, B.-L., Zhao, F., 2016. Effective methods for extracting extracellular polymeric substances from *Shewanella oneidensis* MR-1. *Water Sci. Technol.* 74, 2987–2996.
- Das, T., Sehar, S., Manefield, M., 2013. The roles of extracellular DNA in the structural integrity of extracellular polymeric substance and bacterial biofilm development. *Environ. Microbiol. Rep.* 5, 778–786.
- Do, M.T., Stuckey, D.C., 2019. Fate and removal of Ciprofloxacin in an anaerobic membrane bioreactor (AnMBR). *Bioresour. Technol.* 289.
- Flemming, H.-C., Wingender, J., Szewzyk, U., Steinberg, P., Rice, S.A., Kjelleberg, S., 2016. Biofilms: an emergent form of bacterial life. *Nat. Rev. Microbiol.* 14, 563–575.
- Frolund, B., Griebe, T., Nielsen, P.H., 1995. Enzymatic activity in the activated-sludge floc matrix. *Appl. Microbiol. Biotechnol.* 43, 755–761.
- Gao, L., Lu, X., Liu, H., Li, J., Li, W., Song, R., Wang, R., Zhang, D., Zhu, J., 2019. Mediation of extracellular polymeric substances in microbial reduction of hematite by *Shewanella oneidensis* MR-1. *Front. Microbiol.* 10.
- Getha, K., Vikineswary, S., Chong, V.C., 1998. Isolation and growth of the phototrophic bacterium *Rhodospseudomonas palustris* strain B1 in sago-starch-processing wastewater. *World J. Microbiol. Biotechnol.* 14, 505–511.
- Ge, H., Liu, Z., 2020. Alleviation of tetrabromobisphenol A toxicity in soybean seedlings by *Rhodospseudomonas palustris* RP1n1. *Arch. Microbiol.* 202, 895–903.
- Gong, A.S., Lanzl, C.A., Cwiertny, D.M., Walker, S.L., 2012. Lack of Influence of Extracellular Polymeric Substances (EPS) Level on Hydroxyl Radical Mediated Disinfection of *Escherichia coli*. *Environ. Sci. Technol.* 46, 241–249.
- Guo, Y., Guo, Z., Wang, J., Ye, Z., Zhang, L., Niu, J., 2022. Photodegradation of three antidepressants in natural waters: Important roles of dissolved organic matter and nitrate. *Sci. Total Environ.* 802.
- Hanna, N., Sun, P., Sun, Q., Li, X., Yang, X., Ji, X., Zou, H., Ottoson, J., Nilsson, L.E., Berglund, B., Dyar, O.J., Tamhankar, A.J., Lundborg, C.S., 2018. Presence of antibiotic residues in various environmental compartments of Shandong province in eastern China: Its potential for resistance development and ecological and human risk. *Environ. Int.* 114, 131–142.
- He, H., Han, F., Sun, S., Deng, H., Huang, B., Pan, X., Dionysiou, D.D., 2020. Photosensitive cellular polymeric substances accelerate 17 alpha-ethinylestradiol photodegradation. *Chem. Eng. J.* 381.
- He, H., Xiong, D., Han, F., Xu, Z., Huang, B., Pan, X., 2018. Dissolved oxygen inhibits the promotion of chlorothalonil photodegradation mediated by humic acid. *J. Photochem. Photobiol. a-Chem.* 360, 289–297.
- Hou, R., Gan, L., Guan, F., Wang, Y., Li, J., Zhou, S., Yuan, Y., 2021. Bioelectrochemically enhanced degradation of bisphenol S: mechanistic insights from stable isotope-assisted investigations. *Iscience* 24.
- Hou, R., Luo, X., Liu, C., Zhou, L., Wen, J., Yuan, Y., 2019. Enhanced degradation of triphenyl phosphate (TPHP) in bioelectrochemical systems: Kinetics, pathway and degradation mechanisms. *Environ. Pollut.* 254.
- Hou, R., Luo, C., Zhou, S., Wang, Y., Yuan, Y., Zhou, S., 2020. Anode potential-dependent protection of electroactive biofilms against metal ion shock via regulating extracellular polymeric substances. *Water Res.* 178.
- Huang, W., Yang, F., Huang, W., Lei, Z., Zhang, Z., 2019. Enhancing hydrogenotrophic activities by zero-valent iron addition as an effective method to improve sulfadiazine removal during anaerobic digestion of swine manure. *Bioresour. Technol.* 294.
- Hu, Y., Jiang, L., Zhang, T., Jin, L., Han, Q., Zhang, D., Lin, K., Cui, C., 2018. Occurrence and removal of sulfonamide antibiotics and antibiotic resistance genes in conventional and advanced drinking water treatment processes. *J. Hazard. Mater.* 360, 364–372.
- Igarashi, N., Onoue, S., Tsuda, Y., 2007. Photoreactivity of amino acids: Tryptophan-induced photochemical events via reactive oxygen species generation. *Anal. Sci.* 23, 943–948.
- Karygianni, L., Ren, Z., Koo, H., Thurnheer, T., 2020. Biofilm matrixome: extracellular components in structured microbial communities. *Trends Microbiol.* 28, 668–681.
- Kim, H.J., Park, H.S., Hyun, M.S., Chang, I.S., Kim, M., Kim, B.H., 2002. A mediator-less microbial fuel cell using a metal reducing bacterium, *Shewanella putrefaciens*. *Enzym. Microb. Technol.* 30, 145–152.

- Kong, F., Wang, A., Ren, H.-Y., Huang, L., Xu, M., Tao, H., 2014. Improved dechlorination and mineralization of 4-chlorophenol in a sequential biocathode-bioanode bioelectrochemical system with mixed photosynthetic bacteria. *Bioresour. Technol.* 158, 32–38.
- Korytowski, W., Pilas, B., Sarna, T., Kalyanaraman, B., 1987. Photoinduced generation of hydrogen peroxide and hydroxyl radicals in melanins. *Photochem. Photobiol.* 45, 185–190.
- Kouzuma, A., Meng, X.-Y., Kimura, N., Hashimoto, K., Watanabe, K., 2010. Disruption of the putative cell surface polysaccharide biosynthesis gene SO3177 in *Shewanella oneidensis* MR-1 enhances adhesion to electrodes and current generation in microbial fuel cells. *Appl. Environ. Microbiol.* 76, 4151–4157.
- Kumar, A., Hsu, L.H.-H., Kavanagh, P., Barriere, F., Lens, P.N.L., Lapinonniere, L., Lienhard, J.H., Schroeder, U., Jiang, X., Leech, D., 2017. The ins and outs of microorganism-electrode electron transfer reactions. *Nat. Rev. Chem.* 1.
- Langbehn, R.K., Michels, C., Soares, H.M., 2021. Antibiotics in wastewater: From its occurrence to the biological removal by environmentally conscious technologies. *Environ. Pollut.* 275.
- Larsson, G., Tornkvist, M., 1996. Rapid sampling, cell inactivation and evaluation of low extracellular glucose concentrations during fed-batch cultivation. *J. Biotechnol.* 49, 69–82.
- Lee, E., Glover, C.M., Rosario-Ortiz, F.L., 2013. Photochemical formation of hydroxyl radical from effluent organic matter: role of composition. *Environ. Sci. Technol.* 47, 12073–12080.
- Li, D.-B., Huang, Y.-X., Li, J., Li, L.-L., Tian, L.-J., Yu, H.-Q., 2017. Electrochemical activities of *Geobacter* biofilms growing on electrodes with various potentials. *Electrochim. Acta* 225, 452–457.
- Li, S.-W., Sheng, G.-P., Cheng, Y.-Y., Yu, H.-Q., 2016. Redox properties of extracellular polymeric substances (EPS) from electroactive bacteria. *Sci. Rep.* 6.
- Li, Z., Zhang, P., Qiu, Y., Zhang, Z., Wang, X., Yu, Y., Feng, Y., 2021. Biosynthetic FeS/BC hybrid particles enhanced the electroactive bacteria enrichment in microbial electrochemical systems. *Sci. Total Environ.* 762.
- Li, T., Zhou, Q., Zhou, L., Yan, Y., Liao, C., Wan, L., An, J., Li, N., Wang, X., 2020. Acetate limitation selects *Geobacter* from mixed inoculum and reduces polysaccharide in electroactive biofilm. *Water Res.* 177.
- Logan, B.E., Rossi, R., Ragab, A., Saikaly, P.E., 2019. Electroactive microorganisms in bioelectrochemical systems. *Nat. Rev. Microbiol.* 17, 307–319.
- Luo, C., Hou, R., Chen, G., Liu, C., Zhou, L., Yuan, Y., 2020. UVC-assisted electrochemical degradation of novel bisphenol analogues with boron-doped diamond electrodes: kinetics, pathways and eco-toxicity removal. *Sci. Total Environ.* 711.
- Maizel, A.C., Remucal, C.K., 2017. Molecular Composition and Photochemical Reactivity of Size-Fractionated Dissolved Organic Matter. *Environ. Sci. Technol.* 51, 2113–2123.
- Mangalgi, K.P., Blaney, L., 2017. Elucidating the stimulatory and inhibitory effects of dissolved organic matter from poultry litter on photodegradation of antibiotics. *Environ. Sci. Technol.* 51, 12310–12320.
- McNeill, K., Canonica, S., 2016. Triplet state dissolved organic matter in aquatic photochemistry: reaction mechanisms, substrate scope, and photophysical properties. *Environ. Sci. -Process. Impacts* 18, 1381–1399.
- Michael, I., Rizzo, L., McArdell, C.S., Manaia, C.M., Merlin, C., Schwartz, T., Dagot, C., Fatta-Kassinos, D., 2013. Urban wastewater treatment plants as hotspots for the release of antibiotics in the environment: A review. *Water Res.* 47, 957–995.
- Myers, C.R., Myers, J.M., 1992. Localization of cytochromes to the outer membrane of anaerobically grown *Shewanella putrefaciens* MR-1. *J. Bacteriol.* 174, 3429–3438.
- O'Flynn, D., Lawler, J., Yusuf, A., Parle-McDermott, A., Harold, D., Mc Cloughlin, T., Holland, L., Regan, F., White, B., 2021. A review of pharmaceutical occurrence and pathways in the aquatic environment in the context of a changing climate and the COVID-19 pandemic. *Anal. Methods* 13, 575–594.
- Pi, S., Li, A., Cui, D., Su, Z., Feng, L., Ma, F., Yang, J., 2019. Biosorption behavior and mechanism of sulfonamide antibiotics in aqueous solution on extracellular polymeric substances extracted from *Klebsiella* sp. *J. Bioresour. Technol.* 272, 346–350.
- Qiao, M., Ying, G.-G., Singer, A.C., Zhu, Y.-G., 2018. Review of antibiotic resistance in China and its environment. *Environ. Int.* 110, 160–172.
- Reis, P.J.M., Reis, A.C., Ricken, B., Kolvenbach, B.A., Manaia, C.M., Corvini, P.F.X., Nunes, O.C., 2014. Biodegradation of sulfamethoxazole and other sulfonamides by *Achromobacter denitrificans* PR1. *J. Hazard. Mater.* 280, 741–749.
- Rosario-Ortiz, F.L., Canonica, S., 2016. Probe compounds to assess the photochemical activity of dissolved organic matter. *Environ. Sci. Technol.* 50, 12532–12547.
- Ryan, C.C., Tan, D.T., Arnold, W.A., 2011. Direct and indirect photolysis of sulfamethoxazole and trimethoprim in wastewater treatment plant effluent. *Water Res.* 45, 1280–1286.
- Scarabotti, F., Rago, L., Buhler, K., Harnisch, F., 2021. The electrode potential determines the yield coefficients of early-stage *Geobacter sulfurreducens* biofilm anodes. *Bioelectrochemistry* 140.
- Shang, J., Chen, J., Shen, Z., Xiao, X., Yang, H., Wang, Y., Ruan, A., 2015. Photochemical degradation of PAHs in estuarine surface water: effects of DOM, salinity, and suspended particulate matter. *Environ. Sci. Pollut. Res. Int.* 22, 12374–12383.
- Sharpless, C.M., 2012. Lifetimes of Triplet Dissolved Natural Organic Matter (DOM) and the Effect of NaBH₄ Reduction on Singlet Oxygen Quantum Yields: Implications for DOM Photophysics. *Environ. Sci. Technol.* 46, 4466–4473.
- Sheng, G.P., Yu, H.Q., 2006. Characterization of extracellular polymeric substances of aerobic and anaerobic sludge using three-dimensional excitation and emission matrix fluorescence spectroscopy. *Water Res.* 40, 1233–1239.
- Song, Z., Zhang, X., Ngo, H.H., Guo, W., Wen, H., Li, C., 2019. Occurrence, fate and health risk assessment of 10 common antibiotics in two drinking water plants with different treatment processes. *Sci. Total Environ.* 674, 316–326.
- Sun, D., Chen, J., Huang, H., Liu, W., Ye, Y., Cheng, S., 2016. The effect of biofilm thickness on electrochemical activity of *Geobacter sulfurreducens*. *Int. J. Hydrog. Energy* 41, 16523–16528.
- Sun, J., Hu, Y., Li, W., Zhang, Y., Chen, J., Deng, F., 2015. Sequential decolorization of azo dye and mineralization of decolorization liquid coupled with bioelectricity generation using a pH self-neutralized photobioelectrochemical system operated with polarity reversion. *J. Hazard. Mater.* 289, 108–117.
- Sun, J., Xu, W., Yuan, Y., Lu, X., Kjellerup, B.V., Xu, Z., Zhang, H., Zhang, Y., 2019. Bioelectrical power generation coupled with high-strength nitrogen removal using a photo-bioelectrochemical fuel cell under oxytetracycline stress. *Electrochim. Acta* 299, 500–508.
- Sun, J., Yang, P., Huang, S., Li, N., Zhang, Y., Yuan, Y., Lu, X., 2020. Enhanced removal of veterinary antibiotic from wastewater by photoelectroactive biofilm of purple anoxygenic phototroph through photosynthetic electron uptake. *Sci. Total Environ.* 713.
- Sun, J., Yang, P., Li, N., Zhao, M., Zhang, X., Zhang, Y., Yuan, Y., Lu, X., Lu, X., 2020. Extraction of photosynthetic electron from mixed photosynthetic consortium of bacteria and algae towards sustainable bioelectrical energy harvesting. *Electrochim. Acta* 336.
- Tan, B., Zhou, S., Wang, Y., Zhang, B., Zhou, L., Yuan, Y., 2019. Molecular insight into electron transfer properties of extracellular polymeric substances of electroactive bacteria by surface-enhanced Raman spectroscopy. *Sci. China-Technol. Sci.* 62, 1679–1687.
- Teng, W., Xu, J., Cui, Y., Yu, J., 2020. Photoelectrocatalytic degradation of sulfadiazine by Ag₃PO₄/MoS₂/TiO₂ nanotube array electrode under visible light irradiation. *J. Electroanal. Chem.* 868.
- Tenorio, R., Fedders, A.C., Strathmann, T.J., Guest, J.S., 2017. Impact of growth phases on photochemically produced reactive species in the extracellular matrix of algal cultivation systems. *Environ. Sci. -Water Res. Technol.* 3, 1095–1108.
- Tian, Y., Wei, L., Yin, Z., Feng, L., Zhang, L., Liu, Y., Zhang, L., 2019. Photosensitization mechanism of algogenic extracellular organic matters (EOMs) in the photo-transformation of chlortetracycline: Role of chemical constituents and structure. *Water Res.* 164.
- Tian, Y., Wei, L., Yin, Z., Feng, L., Zhang, L., Liu, Y., Zhang, L., 2019. Photosensitization mechanism of algogenic extracellular organic matters (EOMs) in the photo-transformation of chlortetracycline: Role of chemical constituents and structure. *Water Res.* 164, 114940.
- Tian, Y., Zou, J., Feng, L., Zhang, L., Liu, Y., 2019. *Chlorella vulgaris* enhance the photodegradation of chlortetracycline in aqueous solution via extracellular organic matters (EOMs): Role of triplet state EOMs. *Water Res.* 149, 35–41.
- Wang, L., Li, Y., Wang, L., Zhu, M., Zhu, X., Qian, C., Li, W., 2018. Responses of biofilm microorganisms from moving bed biofilm reactor to antibiotics exposure: Protective role of extracellular polymeric substances. *Bioresour. Technol.* 254, 268–277.
- Wang, H., Luo, H., Fallgren, P.H., Jin, S., Ren, Z.J., 2015. Bioelectrochemical system platform for sustainable environmental remediation and energy generation. *Biotechnol. Adv.* 33, 317–334.
- Wang, Z., Sheng, H., Xiang, L., Bian, Y., Herzberger, A., Cheng, H., Jiang, Q., Jiang, X., Wang, F., 2022. Different performance of pyrene biodegradation on metal-modified montmorillonite: Role of surface metal ions from a bioelectrochemical perspective. *Sci. Total Environ.* 805.
- Wang, L., You, L., Zhang, J., Yang, T., Zhang, W., Zhang, Z., Liu, P., Wu, S., Zhao, F., Ma, J., 2018. Biodegradation of sulfadiazine in microbial fuel cells: Reaction mechanism, biotoxicity removal and the correlation with reactor microbes. *J. Hazard. Mater.* 360, 402–411.
- Wang, S., Yuan, R., Chen, H., Wang, F., Zhou, B., 2021. Anaerobic biodegradation of four sulfanilamide antibiotics: Kinetics, pathways and microbiological studies. *J. Hazard. Mater.* 416.
- Wan, D., Sharma, V.K., Liu, L., Zuo, Y., Chen, Y., 2019. Mechanistic Insight into the Effect of Metal Ions on Photogeneration of Reactive Species from Dissolved Organic Matter. *Environ. Sci. Technol.* 53, 5778–5786.
- Wu, P., Chen, Z., Zhang, Y., Wang, Y., Zhu, F., Can, B., Wu, Y., Li, N., 2019. Rhodospseudomonas palustris wastewater treatment: Cyhalofop-butyl removal, biochemicals production and mathematical model establishment. *Bioresour. Technol.* 282, 390–397.
- Xiao, Y., Zhang, E., Zhang, J., Dai, Y., Yang, Z., Christensen, H.E.M., Ulstrup, J., Zhao, F., 2017. Extracellular polymeric substances are transient media for microbial extracellular electron transfer. *Sci. Adv.* 3.
- Xiao, Y., Zhao, F., 2017. Electrochemical roles of extracellular polymeric substances in biofilms. *Curr. Opin. Electrochem.* 4, 206–211.
- Xie, P., Chen, C., Zhang, C., Su, G., Ren, N., Ho, S.-H., 2020. Revealing the role of adsorption in ciprofloxacin and sulfadiazine elimination routes in microalgae. *Water Res.* 172.
- Xu, Q., Han, B., Wang, H., Wang, Q., Zhang, W., Wang, D., 2020. Effect of extracellular polymer substances on the tetracycline removal during coagulation process. *Bioresour. Technol.* 309.
- Xu, J., Sheng, G.-P., Ma, Y., Wang, L.-F., Yu, H.-Q., 2013. Roles of extracellular polymeric substances (EPS) in the migration and removal of sulfamethazine in activated sludge system. *Water Res.* 47, 5298–5306.
- Xu, P., Xu, H., Shi, Z., 2018. A novel bio-electro-Fenton process with FeVO₄/CF cathode on advanced treatment of coal gasification wastewater. *Sep. Purif. Technol.* 194, 457–461.
- Yang, G., Huang, L., Yu, Z., Liu, X., Chen, S., Zeng, J., Zhou, S., Zhuang, L., 2019. Anode potentials regulate *Geobacter* biofilms: New insights from the composition and spatial structure of extracellular polymeric substances. *Water Res.* 159, 294–301.

- Yang, K., Ji, M., Liang, B., Zhao, Y., Zhai, S., Ma, Z., Yang, Z., 2020. Bioelectrochemical degradation of monoaromatic compounds: Current advances and challenges. *J. Hazard. Mater.* 398.
- Yang, X., Zheng, X., Wu, L., Cao, X., Li, Y., Niu, J., Meng, F., 2018. Interactions between algal (AOM) and natural organic matter (NOM): Impacts on their photodegradation in surface waters. *Environ. Pollut.* 242, 1185–1197.
- Zhang, L., Johnson, N.W., Liu, Y., Miao, Y., Chen, R., Chen, H., Jiang, Q., Li, Z., Dong, Y., Mahendra, S., 2021. Biodegradation mechanisms of sulfonamides by *Phanerochaete chrysosporium* - Luffa fiber system revealed at the transcriptome level. *Chemosphere* 266.
- Zhang, X., Li, J., Fan, W.-Y., Yao, M.-C., Yuan, L., Sheng, G.-P., 2019. Enhanced photodegradation of extracellular antibiotic resistance genes by dissolved organic matter photosensitization. *Environ. Sci. Technol.* 53, 10732–10740.
- Zhang, Q.-Q., Ying, G.-G., Pan, C.-G., Liu, Y.-S., Zhao, J.-L., 2015. Comprehensive evaluation of antibiotics emission and fate in the river basins of China: source analysis, multimedia modeling, and linkage to bacterial resistance. *Environ. Sci. Technol.* 49, 6772–6782.
- Zhao, Q., Guo, W., Luo, H., Xing, C., Wang, H., Liu, B., Si, Q., Li, D., Sun, L., Ren, N., 2022. Insights into removal of sulfonamides in anaerobic activated sludge system: Mechanisms, degradation pathways and stress responses. *J. Hazard. Mater.* 423.
- Zhao, Z., Zhang, G., Zhang, Y., Dou, M., Li, Y., 2020. Fe₃O₄ accelerates tetracycline degradation during anaerobic digestion: Synergistic role of adsorption and microbial metabolism. *Water Res.* 185.
- Zheng, J., Wang, S., Zhou, A., Zhao, B., Dong, J., Zhao, X., Li, P., Yue, X., 2020. Efficient elimination of sulfadiazine in an anaerobic denitrifying circumstance: Biodegradation characteristics, biotoxicity removal and microbial community analysis. *Chemosphere* 252.
- Zhou, S., Liao, Z., Zhang, B., Hou, R., Wang, Y., Zhou, S., Zhang, Y., Ren, Z.J., Yuan, Y., 2021. Photochemical behavior of microbial extracellular polymeric substances in the aquatic environment. *Environ. Sci. Technol.*
- Zhou, Y., Zou, Q., Fan, M., Xu, Y., Chen, Y., 2020. Highly efficient anaerobic co-degradation of complex persistent polycyclic aromatic hydrocarbons by a bioelectrochemical system. *J. Hazard. Mater.* 381.
- Zhuang, Z., Yang, G., Mai, Q., Guo, J., Liu, X., Zhuang, L., 2020. Physiological potential of extracellular polysaccharide in promoting *Geobacter* biofilm formation and extracellular electron transfer. *Sci. Total Environ.* 741.